# EXPLICIT QUANTUM CIRCUITS FOR BLOCK ENCODINGS OF CERTAIN SPARSE MATRICES

#### A PREPRINT

#### **Daan Camps**

Applied Mathematics and Computational Research Division Lawrence Berkeley National Laboratory Berkeley, CA 94720 dcamps@lbl.gov

#### Lin Lin

Department of Mathematics and Challenge Institute of Quantum Computation
University of California at Berkeley
Applied Mathematics and Computational Research Division
Lawrence Berkeley National Laboratory
Berkeley, CA 94720
linlin@math.berkeley.edu

#### Roel Van Beeumen

Applied Mathematics and Computational Research Division Lawrence Berkeley National Laboratory Berkeley, CA 94720 rvanbeeumen@lbl.gov

#### Chao Yang

Applied Mathematics and Computational Research Division Lawrence Berkeley National Laboratory Berkeley, CA 94720 CYang@lbl.gov

April 15, 2022

## **ABSTRACT**

Many standard linear algebra problems can be solved on a quantum computer by using recently developed quantum linear algebra algorithms that make use of block encoding and quantum eigenvalue I singular value transformations. Block encoding embeds a properly scaled matrix of interest I in a larger unitary transformation I that can be decomposed into a product of simpler unitaries and implemented efficiently on a quantum computer. Although quantum algorithms can potentially achieve exponential speedup in solving linear algebra problems compared to the best classical algorithm, such gain in efficiency ultimately hinges on our ability to construct an efficient quantum circuit for the block encoding of I, which is difficult in general, and not trivial even for well structured sparse matrices. In this paper, we give a few examples on how efficient quantum circuits can be explicitly constructed for some well structured sparse matrices, and discuss a few strategies used in these constructions. We are particularly interested in sparse stochastic matrices that represent random walks on a graph, and show how the block encodings of such matrices yield efficient quantum walks.

*Keywords* quantum linear algebra, block encoding, quantum circuit, quantum eigenvalue transformation, quantum singular value transformation, random walk, quantum walk

## 1 Introduction

In recent years, a new class of quantum algorithms have been developed to solve standard linear algebra problems on quantum computers. These algorithms use the technique of block encoding Low and Chuang [2017, 2019], Gilyén et al. [2019] to embed a properly scaled matrix A of interest in a larger unitary matrix  $U_A$  so that the multiplication of A with a vector x can be implemented by applying the unitary matrix  $U_A$  to a carefully prepared initial state and performing measurements on a subset of qubits. Furthermore, if A is Hermitian, by using the technique of quantum eigenvalue transformation, one can block encode a certain matrix polynomial p(A) by another unitary  $U_{p(A)}$  efficiently Low and Chuang [2017]. This procedure can be generalized to non-Hermitian matrices A using a technique called the quantum singular value transformation Gilyén et al. [2019]. The larger unitary  $U_{p(A)}$  can be decomposed into a product of simpler unitaries consisting of  $2 \times 2$  single qubit unitaries, multi-qubit controlled-NOTs,  $U_A$  and its Hermitian conjugate. Because approximate solutions to many large-scale linear algebra such as linear systems of equations, least squares problems and eigenvalue problems (produced by iterative methods) can often be expressed as  $p(A)v_0$  for some initial vector  $v_0$ , the possibility to block encode p(A) will enable us to solve these problems on a quantum computer that performs unitary transformations only Gilyén et al. [2019], Lin and Tong [2020a,b], Martyn et al. [2021] In this paper, we use the term "quantum linear algebra algorithms" to refer to such block encoding based algorithms for solving linear algebra problems on a quantum computer.

In order to implement these quantum linear algebra algorithms, we need to further express the block encoding matrix  $U_A$  as a product of simpler unitaries, i.e., we need to express  $U_A$  as an efficient quantum circuit. In fact, if classical computers can have access to certain quantum inspired sampling based accesses to A, then the potential quantum speedup may be at most polynomial with respect to the system size (though the speedup can still be significant in practice) Chia et al. [2020], Tang [2021], Gharibian and Gall [2021]. Although, it is suggested in Berry et al. [2015], Childs et al. [2017], Low and Chuang [2017], Gilyén et al. [2019] that such a quantum circuit can be constructed in theory for certain sparse matrices, the proposed construction relies on the availability of "oracles" that can efficiently encode both the nonzero structure of A and numerical values of the nonzero matrix elements. However, for a general sparse matrix A, finding these "oracles" is entirely non-trivial. Even for sparse matrices that have a well defined non-zero structure and a small set of nonzero matrix elements, encoding the structure and matrix elements by efficient quantum circuit is not an easy task.

In this paper, we provide a few pedagogical examples on how to explicitly construct efficient quantum circuits for some well structured sparse matrices. In particular, we will present some general strategies for writing down the oracles for the non-zero structure and non-zero matrix elements of these matrices.

The block encoding of A is far from unique. We will show a few different encoding schemes and the corresponding quantum circuits. In general, the unitary  $U_A$  that block encodes A is non-Hermitian even when A is Hermitian. It is possible to construct a Hermitian  $U_A$  that block encodes a Hermitian A (see e.g. Childs et al. [2017]). Although the general strategies we use to construct quantum circuits that block encode A can be applied to different types of sparse matrices with different nonzero matrix elements, we are particularly interested in sparse matrices that represent random walks on a graph Szegedy [2004], Childs [2010]. These matrices are often called stochastic matrices or Markov chain matrices. They are special due to the stochastic property of the matrix elements, but also special because the way they are used in the so-called quantum walk algorithm, which is a quantum version of the classical random walk algorithm that has some interesting properties. It turns out that a quantum walk can be viewed as a block encoding of a Chebyshev polynomial of the discriminant matrix associated with the stochastic matrix used to describe the corresponding random walk. As a result, there is a special way to block encode the discriminant matrix. There is also an intimate connection between the quantum walk and the construction of a Hermitian block encoding of a Hermitian matrix Childs et al. [2017].

This paper is organized as follows. In section 3, we give a formal definition of block encoding of a matrix A and the possibility of using the quantum eigenvalue transformation to block encode p(A) for some polynomial p(t). In section 4, we discuss how to construct a block encoding circuit for a scaled s-sparse matrix A/s, and give two specific examples. In section 4.3, we show how to construct a Hermitian block encoding circuit for a Hermitian matrix. We discuss the possibility to use the techniques presented in section 4 to construct a circuit for the block encoding of P/s in section 5, where P is a doubly stochastic a matrix associated with a random walk. We show this circuit can be used as a building block to construct a circuit for performing a quantum walk associated with such a random walk. However, there is potential loss of quantum efficiency in such a construction due to the 1/s scaling factor produced in the block encoding schemes used in section 4. An alternative approach that uses a different input model and takes advantage of the stochastic property of a random walk is presented. This approach block encodes P directly instead of P/s. As a result, it allows us to construct a more efficient block encoding for a Chebyshev polynomial of P. In the appendix, we compare this approach to earlier work on constructing efficient quantum circuits for Szegedy quantum walks and

show that they are equivalent. We also present an example to demonstrate the effect of a quantum walk and why it is of interest to block encode a Chebyshev polynomial of P in a quantum walk.

#### 2 Notations and Conventions

Following the standard in the literature of quantum computation, we use the Dirac  $\langle \cdot |$  and  $| \cdot \rangle$  notation to denote row and column vectors. In particular  $|0\rangle$  and  $|1\rangle$  are used to represent  $e_1 = (1\ 0)^T$  and  $e_2 = (0\ 1)^T$  respectively. The tensor product of  $m\ |0\rangle$ 's is denoted by  $|0^m\rangle$ . We use  $|x,y\rangle$  to represent the Kronecker product of  $|x\rangle$  and  $|y\rangle$ , which is also sometimes written as  $|x\rangle\ |y\rangle$  or  $|x,y\rangle$ . The jth column of an  $N\times N$  identity is denoted by  $|j\rangle$  for j=0,1,2...,N-1.

We use letters H, X and Z to represent the Hadamard, Pauli-X and Pauli-Z matrices defined below.

$$H = \frac{1}{\sqrt{2}} \begin{pmatrix} 1 & 1 \\ 1 & -1 \end{pmatrix}, \quad X = \begin{pmatrix} 0 & 1 \\ 1 & 0 \end{pmatrix}, \quad \text{and} \quad Z = \begin{pmatrix} 1 & 0 \\ 0 & -1 \end{pmatrix}. \tag{2.1}$$

These are  $2 \times 2$  unitaries and serve as basic single qubit quantum gates. The  $N \times N$  identity matrix is denoted by  $I_N$ . We sometimes drop the subscript N when the dimension of the identity matrix is clear from the context. We follow the standard convention for drawing quantum circuits with multiple parallel lines covered by several layers of rectangular boxes. Each line corresponds to either a single qubit or multiple qubit depending on how it is labelled, and each box corresponds to a single qubit or multi-qubit gate. A vertical line that connects several horizontal lines and a gate is used to represent a controlled gate. The controlling qubit is marked by either a solid or open circle on the corresponding horizontal line. A commonly used controlled gate is a controlled NOT gate drawn as those shown in fig. 1.

**Figure 1.** Controlled-NOT gates.

Mathematically, these diagrams translate into

$$X \otimes E_1 + I \otimes (I - E_1)$$
, and  $X \otimes E_2 + I \otimes (I - E_2)$ , (2.2)

respectively, where

$$E_1 = e_1 e_1^T = |0\rangle \langle 0| \text{ and } E_2 = e_2 e_2^T = |1\rangle \langle 1|,$$
 (2.3)

if the controlling qubit is a single qubit. A similar expression can be use to denote a multi-qubit controlled NOT gates. We will denote a rotation matrix associated with a rotation angle  $\theta$  by  $R(\theta)$  which is defined as

$$R(\theta) = \begin{pmatrix} \cos \theta & -\sin \theta \\ \sin \theta & \cos \theta \end{pmatrix}. \tag{2.4}$$

This rotation can also be written as  $e^{-i\theta Y}$  where Y is the Pauli Y unitary defined as

$$Y = \begin{pmatrix} 0 & -i \\ i & 0 \end{pmatrix}.$$

# 3 Block encoding and quantum eigenvalue transformation

Block encoding is a technique for embedding a properly scaled nonunitary matrix  $A \in \mathbb{C}^{N \times N}$  into a unitary matrix  $U_A$  of the form

$$U_A = \begin{pmatrix} A & * \\ * & * \end{pmatrix}, \tag{3.1}$$

where \* denotes a matrix block yet to be determined. Applying  $U_A$  to a vector of the form

$$v = \begin{pmatrix} x \\ 0 \end{pmatrix} = |0\rangle |x\rangle \tag{3.2}$$

yields

$$w = U_A v = \begin{pmatrix} Ax \\ * \end{pmatrix} = |0\rangle |Ax\rangle + |1\rangle |*\rangle,$$

where \* here denotes a vector that we do not care about. If we measure the first qubit and obtain the  $|0\rangle$  state, the second qubit then contains  $|Ax\rangle$ . The probability of such a successful measurement is  $||Ax||^2$ .

Note that by "a properly scaled A", we mean that A is scaled to satisfy  $||A||_2 \le 1$ . Without such a scaling, a block encoding of A may not exist. Furthermore, if there are some constraints on the type of unitary we can construct, e.g., the type of quantum gates available on a quantum computer, we may not be able to find a  $U_A$  that block encodes A exactly. However, in this paper, we assume that A has already been properly scaled, and there is no constraints on the quantum gates we can use to construct a quantum circuit representation of the unitary matrix  $U_A$ .

To give an example of block encoding, let us consider a  $1 \times 1$  matrix  $A = (\alpha)$ , where  $0 < \alpha < 1$ . In this extremely simple case, a block encoding of A can be constructed as

$$U_A = \begin{pmatrix} \alpha & \sqrt{1 - \alpha^2} \\ \sqrt{1 - \alpha^2} & -\alpha \end{pmatrix} \text{ or } U_A = \begin{pmatrix} \alpha & -\sqrt{1 - \alpha^2} \\ \sqrt{1 - \alpha^2} & \alpha \end{pmatrix}.$$
(3.3)

Although this type of block encoding can be extended to a properly scaled matrix A of a larger dimension to yield

$$U_{A} = \begin{bmatrix} A & (I - A^{\dagger}A)^{1/2} \\ (I - A^{\dagger}A)^{1/2} & -A \end{bmatrix} \text{ or } \begin{bmatrix} A & -(I - A^{\dagger}A)^{1/2} \\ (I - A^{\dagger}A)^{1/2} & A \end{bmatrix},$$
(3.4)

this approach is not practical because it requires computing the square root of  $A^{\dagger}A$ , which is generally difficult to implement on a quantum computer.

A more practical scheme that does not require computing the square root of A can be illustrated by the following real symmetric  $2 \times 2$  example. Let

$$A = \frac{1}{2} \begin{pmatrix} \alpha_1 & \alpha_2 \\ \alpha_2 & \alpha_1 \end{pmatrix}, \tag{3.5}$$

where  $0 < |\alpha_1|, |\alpha_2| < 1$ . It can be verified that the matrix

$$U_A = \frac{1}{2} \begin{pmatrix} U_{\alpha} & -U_{\beta} \\ U_{\beta} & U_{\alpha} \end{pmatrix} \tag{3.6}$$

is a block encoding of A, where

$$U_{\alpha} = \begin{pmatrix} \alpha_{1} & \alpha_{2} & \alpha_{1} & -\alpha_{2} \\ \alpha_{2} & \alpha_{1} & -\alpha_{2} & \alpha_{1} \\ \alpha_{1} & -\alpha_{2} & \alpha_{1} & \alpha_{2} \\ -\alpha_{2} & \alpha_{1} & \alpha_{2} & \alpha_{1} \end{pmatrix} \text{ and } U_{\beta} = \begin{pmatrix} \beta_{1} & \beta_{2} & \beta_{1} & -\beta_{2} \\ \beta_{2} & \beta_{1} & -\beta_{2} & \beta_{1} \\ \beta_{1} & -\beta_{2} & \beta_{1} & \beta_{2} \\ -\beta_{2} & \beta_{1} & \beta_{2} & \beta_{1} \end{pmatrix},$$
(3.7)

with  $\beta_1 = \sqrt{1 - \alpha_1^2}$  and  $\beta_2 = \sqrt{1 - \alpha_2^2}$ . To implement this unitary on a quantum computer, we must further decompose  $U_A$  as a product of simpler unitaries and construct a quantum circuit with a limited number of quantum gates. We will discuss how to construct such a quantum circuit in the next section. The method for constructing the block encoding shown in (3.6) cannot be easily generalized to matrices of larger dimensions. However, for matrices with special structures, e.g., sparse matrices, it is possible to develop some general block encoding strategies which we will discuss in the next section. The general definition of a block encoding is as follows.

**Definition 3.1** (Block encoding). Given an n-qubit matrix A ( $N=2^n$ ), if we can find  $\alpha, \epsilon \in \mathbb{R}_+$ , and an (m+n)-qubit unitary matrix  $U_A$  so that

$$||A - \alpha \left( \langle 0^m | \otimes I_N \right) U_A \left( |0^m \rangle \otimes I_N \right) ||_2 \le \epsilon, \tag{3.8}$$

then  $U_A$  is called an  $(\alpha, m, \epsilon)$ -block-encoding of A. In particular, when the block encoding is exact with  $\epsilon = 0$ ,  $U_A$  is called an  $(\alpha, m)$ -block-encoding of A.

Here m is the number of ancilla qubits used to block encode A, and the expression  $(\langle 0^m | \otimes I_N \rangle U_A (|0^m \rangle \otimes I_N)$  should be interpreted as taking the upper-left  $2^n \times 2^n$  matrix block of  $U_A$ . For example, the block encoding in Equation (3.6) is a (1,2)-block-encoding of A in Equation (3.5).

When solving a large and sparse linear algebra problem on a classical computer, we often use an iterative solver to seek an approximate solution  $\hat{x}$ . For simplicity we assume A is Hermitian. In many cases (such as when a Krylov subspace method is used), the approximate solution can be written as  $\hat{x} = p(A)v_0$ , where p(t) is a polynomial that approximates a desired function and  $v_0$  is an initial guess or simply a random vector. For example, to solve a linear system of equations Ax = b, we choose p(t) to be a polynomial approximation to 1/t on the spectrum of A.

To solve this problem on a quantum computer using the technique of block encoding, we need to block encode the matrix function p(A). If we are provided a (1, m)-block-encoding of the Hermitian matrix A denoted by  $U_A$ , this task

can be achieved by a quantum eigenvalue transformation Low and Chuang [2017], Gilyén et al. [2019]. Specifically, for any real polynomial p(t) of degree d satisfying (1) the parity of p is  $(d \mod 2)$ , and (2)  $|p(t)| \leq 1, \forall t \in [-1,1]$ , there exists a set of parameters  $\{\phi_i\}_{i=0}^d \in \mathbb{R}^{d+1}$  so that the quantum circuit in fig. 2 provides a (1, m+1)-block-encoding of p(A) [Gilyén et al., 2019, Corollary 11] denoted by  $U_{p(A)}$ .

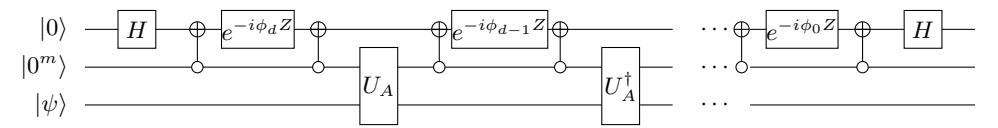


**Figure 2.** A quantum circuit for the block encoding of p(A).

The phase angles  $\phi_0$ ,  $\phi_1$ , ...,  $\phi_d$  appeared in fig. 2 are completely determined by the polynomial p(t), and the set of phase angles is generally not unique. They can be computed using analytic methods (but potentially requiring extended precision arithmetic operations) Gilyén et al. [2019], Haah [2019], or optimization based methods Dong et al. [2021] (with standard double precision arithmetic operations).

Once we have an efficient quantum circuit to construct the block encoding  $U_A$ , we can easily construct an efficient quantum circuit for  $U_{p(A)}$ . For a general matrix A, the quantum circuit in fig. 2 no longer corresponds to a quantum eigenvalue transformation, but a quantum singular value transformation (QSVT) of A (see Gilyén et al. [2019] for more detailed discussion of QSVT). In the next section, we will focus on techniques for constructing an efficient quantum circuit for  $U_A$  associated with a well structured sparse A.

## 4 Efficient quantum circuit for the block encoding of an s-sparse matrix

The block encoding (3.6) for the  $2 \times 2$  matrix (3.5) can be factored as a product of simpler unitaries, i.e.,

$$U_A = [I_2 \otimes H \otimes I_2] [R_1 \otimes I_2 \otimes I_2] [(I_2 \otimes E_1 + R_2 \otimes E_2) \otimes I_2]$$
$$[I_2 \otimes (E_1 \otimes I_2 + E_2 \otimes X)] \otimes [I_2 \otimes H \otimes I_2], \quad (4.1)$$

where H, X are the Hadamard and Pauli-X gates defined in (2.1),  $E_1$  and  $E_2$  are projectors defined in (2.3), and  $R_1 = R(\theta_1)$  and  $R_2 = R(\theta_2)$  are rotation matrices associated with the angles  $\theta_1 = \arccos(\alpha_1)$  and  $\theta_2 = \arccos(\alpha_2) - \theta_1$ .

The quantum circuit associated with the factorization given in (4.1) is shown in fig. 3. Note that in this case, the quantum

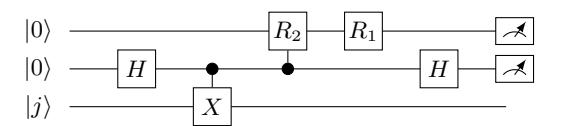


**Figure 3.** A quantum circuit for the block encoding of a  $2 \times 2$  symmetric matrix A.

circuit requires 2 ancilla qubits in addition to the n=1 system qubit required to match the dimension of A, which is  $N=2^n$ . As a result, the unitary that block encodes the  $2\times 2$  matrix A has a dimension of  $2^3$ , which is two times larger than the dimension of the block encoding given by (3.4).

Although it is difficult to generalize the block encoding scheme for the  $2 \times 2$  matrix (3.5) and the corresponding quantum circuit to a block encoding scheme for an arbitrary  $N \times N$  matrix A, it is possible to develop such a scheme for well structured matrices. In particular, when the matrix A is sparse with a structured sparsity pattern and the nonzero matrix elements can also be well characterized, an efficient block encoding of A can be constructed.

In the following, we will focus on an s-sparse matrix, which is defined to be an sparse matrix with at most s nonzeros in each column and row. For simplicity, let us assume  $s=2^m \ll N$  for some integer  $m \ll n$ . When s is not a power of 2, we can always increase s to a power of 2 by treating some zeros as nonzeros. The following theorem, which is a variant of [Gilyén et al., 2019, Lemma 48 (in the full version)], asserts that such a sparse matrix can be block encoded if we can construct unitaries that can encodes both the nonzero structure and the non-zero matrix elements of A.

**Theorem 4.1.** Let  $c(j,\ell)$  be a function that gives the index of the  $\ell$ th non-zero element in the jth column of an s-sparse matrix  $A \in \mathbb{C}^{N \times N}$  with  $N = 2^n$ , where  $s = 2^m$ . If there exists a unitary  $O_c$  such that

$$O_c |\ell\rangle |j\rangle = |\ell\rangle |c(j,\ell)\rangle,$$
 (4.2)

and a unitary  $O_A$  such that

$$O_A |0\rangle |\ell\rangle |j\rangle = \left( A_{c(j,\ell),j} |0\rangle + \sqrt{1 - |A_{c(j,\ell),j}|^2} |1\rangle \right) |\ell\rangle |j\rangle , \tag{4.3}$$

then

$$U_A = (I_2 \otimes D_s \otimes I_N) (I_2 \otimes O_c) O_A (I_2 \otimes D_s \otimes I_N),$$

$$(4.4)$$

where  $D_s$  is a diffusion operator defined as

$$D_s |0^m\rangle = \frac{1}{\sqrt{s}} \sum_{\ell=0}^{s-1} |\ell\rangle, \qquad (4.5)$$

with  $|\ell\rangle$  understood to be a computational basis in the Hilbert space defined by m qubits, block encodes A/s.

*Proof.* Our goal is to show that  $\langle 0|\langle 0^m|\langle i|U_A|0\rangle|0^m\rangle|j\rangle=A_{ij}/s$ . In order to compute the inner product  $\langle 0|\langle 0^m|\langle i|U_A|0\rangle|0^m\rangle|j\rangle$ , we apply  $D_s,O_A,O_c$  to the  $|0\rangle|0^m\rangle|j\rangle$  successively as illustrated below

$$|0\rangle |0^{m}\rangle |j\rangle \xrightarrow{D_{s}} \frac{1}{\sqrt{s}} \sum_{\ell \in [s]} |0\rangle |\ell\rangle |j\rangle$$

$$\xrightarrow{O_{A}} \frac{1}{\sqrt{s}} \sum_{\ell \in [s]} \left( A_{c(j,\ell),j} |0\rangle + \sqrt{1 - |A_{c(j,\ell),j}|^{2}} |1\rangle \right) |\ell\rangle |j\rangle$$

$$\xrightarrow{O_{c}} \frac{1}{\sqrt{s}} \sum_{\ell \in [s]} \left( A_{c(j,\ell),j} |0\rangle + \sqrt{1 - |A_{c(j,\ell),j}|^{2}} |1\rangle \right) |\ell\rangle |c(j,\ell)\rangle.$$

$$(4.6)$$

Instead of multiplying the last factor  $I_2 \otimes D_s \otimes I_N$  in (4.4) to last line of (4.6), we apply it to  $|0\rangle |0^m\rangle |i\rangle$  first to obtain

$$|0\rangle |0^{m}\rangle |i\rangle \xrightarrow{D_{s}} \frac{1}{\sqrt{s}} \sum_{\ell' \in [s]} |0\rangle |\ell'\rangle |i\rangle.$$
 (4.7)

Finally, taking the inner product between (4.6) and (4.7) yields

$$\langle 0|\langle 0^m|\langle i|U_A|0\rangle|0^m\rangle|j\rangle = \frac{1}{s}\sum_{\ell}A_{c(j,\ell),j}\delta_{i,c(j,\ell)} = \frac{1}{s}A_{ij}.$$
(4.8)

The quantum circuit associated with the block encoding defined in theorem 4.1 is shown in fig. 4. Note that the implementation of this block encoding requires m+1 ancilla qubits in addition to n system qubits. In order to turn this into an efficient quantum circuit, we need to decompose the  $D_s$ ,  $O_c$  and  $O_A$  unitaries into a sequence of quantum gates. The decomposition for  $D_s$  is relatively easy. We can simply set  $D_s$  to  $H^{\otimes m}$ , with H defined by (2.1). Constructing efficient quantum circuits for  $O_A$  and  $O_C$  is generally much harder. Although it may be possible to construct a set of controlled quantum gates to achieve (4.2) and (4.3) for a specific pair of j and  $\ell$ . This approach will not yield an efficient quantum circuit because the total number of quantum gates in the circuit will be on the order of  $\mathcal{O}(N)$ , which is exponential with respect to n. Our goal is to construct a circuit that has a gate complexity of  $\operatorname{poly}(n)$ , i.e., a polynomial in n, at least for certain sparse matrices with well defined sparsity patterns.

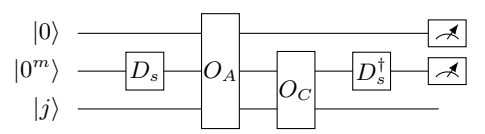


**Figure 4.** A general schematic circuit drawing for the block encoding of an s-sparse matrix

Note that  $O_C$  is unitary. According to eq. (4.2), we must have  $O_C^\dagger |\ell\rangle |c(j,\ell)\rangle = |\ell\rangle |j\rangle$ . This means that for each row index  $i=c(j,\ell)$ , we can recover the column index j given the value of  $\ell$ . This assumption is of course somewhat restrictive, but it covers important cases such as banded matrices. For more general query models we refer readers to Gilyén et al. [2019]. We remark that it can generally be more difficult to explicitly construct quantum circuits for  $O_C$ 's in these more general query models.

In the following, we give some specific examples to illustrate how efficient quantum circuits for  $O_C$  and  $O_A$  can be constructed for some well structured sparse matrices.

#### 4.1 Banded circulant matrix

A sparse matrix A can be viewed as an adjacency matrix for a directed graph defined in terms a vertex set V, which consists of column indices  $\{j\}$  of A, and an edge set E, which consists of pairs of indices  $\{(i,j)\}$ . The (i,j)th element of A is nonzero if  $(i,j) \in E$ . The numerical value of the (i,j)th element of A, denoted by  $A_{i,j}$ , represents the weight of the edge emanating from the vertex j and incident to the vertex i for a directed graph. For an undirected graph, the corresponding adjacency matrix is symmetric, i.e.,  $A_{i,j} = A_{j,i}$ .

In this section, we will focus on the sparse matrix associated with a directed cyclic graph. To illustrate this, we consider the following cyclic graph with N=8 vertices and associated banded circulant adjacency matrix

$$A = \begin{pmatrix} \alpha & \gamma & 0 & \cdots & \beta \\ \beta & \alpha & \ddots & \ddots & 0 \\ 0 & \beta & \ddots & \gamma & \vdots \\ \vdots & \ddots & \ddots & \alpha & \gamma \\ \gamma & 0 & \cdots & \beta & \alpha \end{pmatrix}. \tag{4.9}$$

For each vertex  $j, 0 \le j \le N-1$ , there are two directed edges emanating from j, i.e.,  $(\operatorname{mod}(j-1,N),j) \in E$  and  $(j,\operatorname{mod}(j+1,N)) \in E$ . The weights associated with these edges are  $\beta$  and  $\gamma$ . We also assign a weight  $\alpha$  to each vertex. This weight can also be viewed as the weight associated with a self-loop edge from a vertex j to itself. The matrix is nearly tridiagonal with the value  $\alpha$  on its diagonal,  $\gamma$  on its superdiagonal and  $\beta$  on the subdiagonal. The non-zero elements  $A_{N-1,0} = \gamma$  and  $A_{0,N-1} = \beta$  reflect the cyclic feature of the graph. Each column of the matrix has 3 nonzeros. We use  $\lceil \log_2 3 \rceil = 2$  ancilla qubits to encode the row indices of the nonzero matrix elements in each column. An additional ancilla qubit is needed to encode the numerical values of the nonzero matrix elements.

#### **4.1.1** The $O_C$ circuit

For the adjacency sparse matrix induced by the cyclic graph, the function  $c(j, \ell)$ , which defines the row index of the  $\ell$ th nonzero element in the jth column is relatively easy to define, i.e., it can be written as

$$c(j,\ell) = \text{mod}(j+\ell-1,N).$$
 (4.10)

Therefore, to implement the  $O_C$  unitary defined in (4.2), we need to construct a circuit to map  $|j\rangle$  to  $|\text{mod}(j-1,N)\rangle$  or  $|\text{mod}(j+1,N)\rangle$  depending on the value of  $\ell$ . These cyclic addition and subtraction mappings are simply right and left shift permutation operators defined as

$$R = \begin{pmatrix} 0 & 1 & \dots & 0 \\ 0 & 0 & 1 & \ddots & 0 \\ \vdots & \ddots & \ddots & \ddots & \vdots \\ \vdots & \ddots & \ddots & \ddots & 1 \\ 1 & 0 & \dots & \ddots & 0 \end{pmatrix}, \text{ and } L = \begin{pmatrix} 0 & 0 & \dots & 1 \\ 1 & 0 & 0 & \ddots & 0 \\ \vdots & 1 & \ddots & \ddots & \vdots \\ \vdots & \ddots & \ddots & \ddots & \vdots \\ 0 & 0 & \dots & 1 & 0 \end{pmatrix}. \tag{4.11}$$

Note that the L and R gates correspond to the addition and subtraction arithmetic operations (i.e., +1 or -1), respectively. They can be implemented by a quantum circuit consisting of multi-qubit controlled-NOT gates shown in figs. 5a and 5b. The multi-qubit controlled gates perform the carry operation in the binary format (see e.g. [Rieffel and Polak, 2011, Chapter 6]).



**Figure 5.** The shift circuits

To use these shift components in the quantum circuit implementation of  $O_C$ , we need to control the applications of the L and R shift operators from the qubits used to represent  $|\ell\rangle$ . We always apply the R-shift to account for the -1 term in (4.10). For  $\ell=0$ , nothing else needs to be done. For  $\ell=1$ , we need to apply the L-shift to offset the R-shift so that  $|j\rangle$  is mapped to itself (the diagonal element). For  $\ell=2$ , we need to apply L-shift twice to encode the row index of the subdiagonal elements. Note that the use of  $D_s$  requires us to consider also  $\ell=3$  even though the matrix A only has 3 nonzero elements per column. In this case, we need to apply R-shift twice to offset the applications of both L and  $L^2$  controlled by the first and second qubits. All of these conditions can be implemented by the  $O_C$  circuit shown in fig. 6.

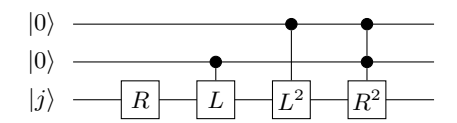


**Figure 6.** A quantum circuit for the  $O_C$  operator.

If we use  $L_3$  to denote a 3-qubit L-shift operator of size  $8 \times 8$ , then it can be shown that

$$L_3^2 = L_2 \otimes I_2, \tag{4.12}$$

where  $L_2$  is a  $4 \times 4$  2-qubit L-shift operator. As a result, the circuit for the  $L_3^2$ -shift operator can be drawn as in fig. 7. A similar decomposition holds for  $R_8^2$ .

Figure 7.  $L^2$ -shift circuit

Note that the construction of  $O_C$  depends on how  $c(j,\ell)$  is defined, which is not unique. For example, instead of defining  $c(j,\ell)$  by (4.10), we can use the following definition

$$c(j,\ell) = \begin{cases} j & \text{if } \ell = 0 \text{ (diagonal) or 3,} \\ j+1 & \text{if } \ell = 1 \text{ (subdiagonal),} \\ j-1 & \text{if } \ell = 2 \text{ (supdiagonal).} \end{cases}$$

$$(4.13)$$

Such a definition yields a simpler  $O_C$  circuit shown in fig. 8.

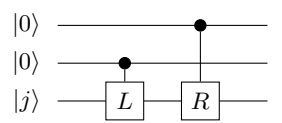


**Figure 8.** An alternative quantum circuit for the  $O_C$  operator using (4.13) for  $c(j,\ell)$ .

## **4.1.2** The $O_A$ circuit

The basic strategy to construct a circuit for  $O_A$  defined by (4.3) is to use controlled rotations to place nonzero values at proper locations in  $U_A$ . As we have already seen that the unitary  $U_A$  defined in (3.3) is a block encoding of a scalar  $\alpha$ , with  $0 \le |\alpha| \le 1$ . It is in fact a rotation matrix  $R(\theta)$  with  $\theta \equiv \arccos \alpha$ . To construct a circuit for (4.3), we need to condition the application of such a rotation on the values of j and  $\ell$  in general. For circulant matrices, the matrix elements of A depend exclusively on  $\ell$ . Therefore, we only place control on qubits used to represent  $|\ell\rangle$ . The rotation angle is a function of  $\ell$  also.

If we choose to use (4.13) to define  $c(j, \ell)$ , we can encode the diagonal of A by using

$$O_A^{(1)} = R(\theta_1) \otimes E_1 \otimes E_1 + R(\pi/2) \otimes (I_4 - E_1 \otimes E_1),$$
 (4.14)

where  $\theta_1 = \arccos \alpha$ . It is easy to verify that

$$\left(O_A^{(1)} \otimes I_8\right) \left(I_2 \otimes D_s \otimes I_8\right) |0\rangle |00\rangle |j\rangle = \frac{1}{\sqrt{2}} \left(O_A^{(1)} \otimes I_8\right) |0\rangle \left(|00\rangle + |01\rangle + |10\rangle + |11\rangle\right) |j\rangle 
= \frac{1}{\sqrt{2}} R(\theta_1) |0\rangle |00\rangle |j\rangle.$$
(4.15)

Applying  $O_C$  defined by the circuit in fig. 8 to (4.15) does not alter it. Finally, taking the inner product of (4.15) with  $(I_2 \otimes D_s \otimes I_8) |0\rangle |0\rangle |j\rangle$  results in  $(\langle 0|R(\theta_1)|0\rangle)/2 = \cos(\theta_1)/2 = \alpha/2$ .

The subdiagonal and superdiagonal of A can then be encoded by

$$O_A^{(2)} = R(\theta_2) \otimes E_1 \otimes E_2 + I_2 \otimes (I_4 - E_1 \otimes E_2), \tag{4.16}$$

and

$$O_A^{(3)} = R(\theta_3) \otimes E_1 \otimes E_2 + I_2 \otimes (I_4 - E_1 \otimes E_2), \tag{4.17}$$

 $O_A^{(3)} = R(\theta_3) \otimes E_1 \otimes E_2 + I_2 \otimes (I_4 - E_1 \otimes E_2),$  (4.17) where  $\theta_2 = \arccos \beta - \pi/2$  and  $\theta_3 = \arccos \gamma - \pi/2$ . The subtractions of  $\pi/2$  from  $\arccos \beta$  and  $\arccos \gamma$  are performed to account for the  $R(\pi/2)$  performed in (4.14) for  $\ell \neq 0$ .

Combining  $O_A^{(1)}$ ,  $O_A^{(2)}$  and  $O_A^{(3)}$  yields the  $O_A = O_A^{(3)} \cdot O_A^{(2)} \cdot O_A^{(1)}$  circuit shown in fig. 9.

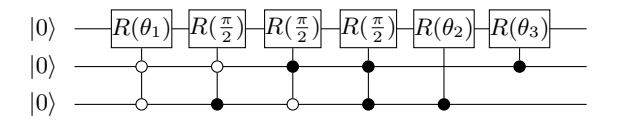


**Figure 9.** An example of the  $O_A$  circuit for  $8 \times 8$  banded circulant matrix.

There are multiple ways to construct the  $O_A$  circuit also. The three controlled  $\pi/2$  rotations can be removed if we define  $O_A^{(1)}$  as

$$O_A^{(1)} = R(\theta_1) \otimes E_1 \otimes E_1 + I \otimes (I_4 - E_1 \otimes E_1).$$
 (4.18)

 $O_A^{(1)} = R(\theta_1) \otimes E_1 \otimes E_1 + I \otimes (I_4 - E_1 \otimes E_1).$  (4.18) However, in this case, we need to change the angle  $\theta_1$  to  $\theta_1 = \arccos(\alpha - 1)$ . To see why this is the case, we apply  $O_A^{(1)}\otimes I_8$  again to  $(I_2\otimes D_s\otimes I_8)\ket{0}\ket{00}\ket{j}$ . The result of this operation is

$$\frac{1}{\sqrt{2}} \left[ R(\theta_1) \left| 0 \right\rangle \left| 00 \right\rangle + \left| 0 \right\rangle \left| 01 \right\rangle + \left| 0 \right\rangle \left| 10 \right\rangle + \left| 0 \right\rangle \left| 11 \right\rangle \right] \left| j \right\rangle \tag{4.19}$$

Applying the  $O_C$  circuit to (4.19) yields

$$\frac{1}{\sqrt{2}} \left[ (R(\theta_1) |0\rangle |00\rangle + |0\rangle |11\rangle) |j\rangle + |0\rangle |01\rangle |j+1\rangle + |0\rangle |10\rangle |j-1\rangle \right]. \tag{4.20}$$

Taking the inner product of (4.20) with  $(I_2 \otimes D_s \otimes I_8) |0\rangle |00\rangle |j\rangle$  results in  $[\cos(\theta_1) + 1]/2$ . Therefore, to satisfy  $[\cos(\theta_1) + 1]/2 = \alpha/2$ , we set  $\theta_1$  to  $\theta_1 = \arccos(\alpha - 1)$ .

Removing the controlled  $\pi/2$  rotations also results in modifications of  $\theta_2$  and  $\theta_3$  to  $\theta_2 = \arccos \beta$  and  $\theta_3 = \arccos \gamma$ respectively.

#### 4.1.3 The complete circuit

The complete circuit for a block encoding of A/2 for a  $8 \times 8$  circulant matrix of the form (4.9) is given in fig. 10. The total number of Hadamard gates and controlled rotations are proportional to log(s) which is generally very small for a sparse matrix. The number of controlled R and L shifts is also on the order of  $O(\log s)$ . Each controlled-R and controlled-L circuit is a general multi-qubit controlled (Toffoli) gate that can be further decomposed into poly(n)two-qubit gates. Therefore, the overall gate complexity of the  $U_A$  circuit is poly(n), which is considered efficient.

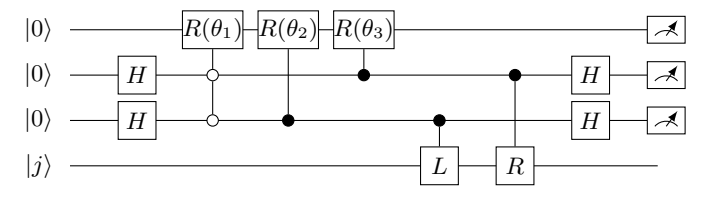


**Figure 10.** A complete quantum circuit for the block encoding of a  $8 \times 8$  banded circulant matrix with  $\theta_1 = \arccos(\alpha - 1)$ ,  $\theta_2 = \arccos(\beta)$  and  $\theta_3 = \arccos(\gamma)$ .

We should also note that the circuit shown in fig. 10 can be easily modified to block encode a tridiagonal matrix with  $\alpha$  on the diagonal,  $\beta$  on the subdiagonal and  $\gamma$  on the superdiagonal. All we need to do is to add the following two multi-qubit control gates to the sequence of gates in the  $O_A$  block of the circuit. These gates perform controlled rotations  $R(\theta_5)$  and  $R(\theta_6)$  to zero out  $\gamma$  in the (N-1,0)th entry of  $U_A$  and  $\beta$  in the (0,N-1)th entry of  $U_A$  respectively. The rotation angles  $\theta_5$  and  $\theta_6$  should be set to  $\theta_5 = \pi/2 - \arccos(\beta)$  and  $\theta_6 = \pi/2 - \arccos(\gamma)$  respectively.

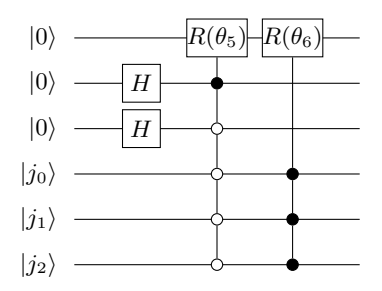


**Figure 11.** Multi-qubit controlled rotations that can be added to the quantum circuit shown in fig. 10 to block encode a tri-diagonal matrix.

## 4.2 Extended binary tree

The banded circulant matrix is special in the sense that the  $c(j,\ell)$  function is relatively simple, and the values of nonzero matrix elements are independed of j. Next we consider another special case that has a slightly more complicated  $c(j,\ell)$  function. In this case, the matrix A is the adjacency matrix for an undirected and balanced binary tree. A standard balanced binary tree has  $2^n-1$  vertices. To simplify our discussion, we add one additional vertex and connect it to the root of the binary tree so that the total number of vertices is  $2^n$ . The additional vertex is the new root of the tree and labeled by 0. We call this binary tree an extended binary tree and consider the following extended binary tree with 8 vertices and associated  $8 \times 8$  adjacency matrix

$$A = \begin{pmatrix} \gamma & \beta & & & & & \\ \beta & \alpha & \beta & \beta & & & & \\ \beta & \alpha & \beta & \beta & & & & \\ \beta & \alpha & & \beta & \beta & & & \\ \beta & \alpha & & \beta & \beta & & & \\ \beta & \alpha & & \gamma & & & \\ \beta & \alpha & \alpha & & \gamma & & \\ \beta & \alpha & \alpha & \alpha & & \\ \beta & \alpha & \alpha & \alpha & & \\ \beta & \alpha & \alpha & \alpha & & \\ \beta & \alpha & \alpha & \alpha & & \\ \beta & \alpha & \alpha & \alpha & & \\ \beta & \alpha & \alpha & \alpha & & \\ \beta & \alpha & \alpha & \alpha & & \\ \beta & \alpha & \alpha & \alpha & & \\ \beta & \alpha & \alpha & \alpha & & \\ \beta & \alpha & \alpha & \alpha & & \\ \beta & \alpha & \alpha & \alpha & & \\ \beta & \alpha & \alpha & \alpha & & \\ \beta$$

We assign the weight  $0 < \alpha < 1$  to each vertex (or self loop from a vertex to itself) with the exception of the root and leaves of the tree. For those vertices, we assign the weight  $0 < \gamma < 1$  instead. We assign the weight  $0 < \beta < 1$  to each edge between a parent and its child. Furthermore, the weights  $\alpha$ ,  $\beta$  and  $\gamma$  are chosen to ensure ||A|| < 1.

The function  $c(j,\ell)$  associated with the nonzero pattern of this matrix can be defined as

$$c(j,\ell) = \begin{cases} j & \text{if } \ell = 0 \text{ (diagonal);} \\ 2j & \text{if } \ell = 1 \text{ (left child);} \\ 2j+1 & \text{if } \ell = 2 \text{ (right child);} \\ \lfloor j/2 \rfloor & \text{if } \ell = 3 \text{ (parent);} \end{cases}$$

$$(4.22)$$

Note that this function is only correct for columns associated with internal vertices (vertices that are neither the root nor the leaves) of the binary tree, which has four non-zero matrix elements per column. For columns associated with the root and leaf vertices, which has only two non-zeros matrix elements per column, this function creates some "spurious" non-zero row indices. However, we can construct proper controlled rotations in  $O_A$  to zero out matrix elements associated with these row indices.

## **4.2.1** The $O_C$ circuit

Because the function  $c(j, \ell)$  defined in (4.22) involves multiplying a column index j by 2 and dividing j by 2, the  $O_C$  circuit will contain controlled subcircuits that perform these operations in addition to the controlled L-shift circuit used to perform the addition by 1 for  $\ell = 2$ .

The mapping from  $|j\rangle$  to  $|2j\rangle$  can be defined by a unitary operator  $M_2$  which consists of a sequence of swap operations between adjacency qubits as shown in fig. 12. Note that the bottom 3 qubits are used to encode the column index with  $|j_0\rangle$  being the label for the least significant and  $|j_2\rangle$  being the label for the most significant bits. The top qubit labelled by  $|0\rangle$  is an ancilla qubit that serves as a carry for  $j \geq 4$ . However, since j is a leave vertex for  $j \geq 4$ , we do not need the correct evaluation of 2j for these indices. Therefore, we can in principle leave out the ancilla qubit in fig. 12.

The mapping from j to  $\lfloor j/2 \rfloor$ , which we denote by  $D_2$ , is the inverse operation of  $M_2$ . Thus, we can simply reverse the sequence of SWAP gates in fig. 12 to obtain a circuit for  $D_2$ . Note that in this case, we do need to keep the ancilla qubit

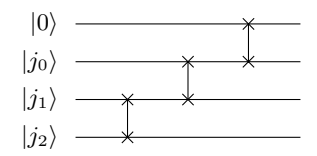


**Figure 12.** The quantum circuit for multiplying  $|j\rangle$  by 2.

labelled by  $|0\rangle$ . It is easy to verify that this circuit performs the correct mapping for both odd and even j's. However, for odd j's, the ancilla qubit will be set to  $|1\rangle$  after  $D_2$  is applied. This is problematic because in that case the inner product  $(\langle 0|\langle i|)D_2(|0\rangle|j\rangle)$ , which appears in the evaluation of the (i,j)th element of  $U_A$ , becomes  $(\langle 0|\langle i|)(|1\rangle||j/2]\rangle)=0$ . Consequently, we cannot properly encode the non-zero element  $A_{i,j}$  when i is the parent of j and j is odd. However, this problem can be resolved by applying a Hadamard gate on the ancilla qubit to ensure that its state contains a nonzero component in the  $|0\rangle$  direction after  $O_C$  is applied. With properly constructed  $M_2$  and  $D_2$  circuits, we can draw the  $O_C$  circuit as shown in fig. 13.

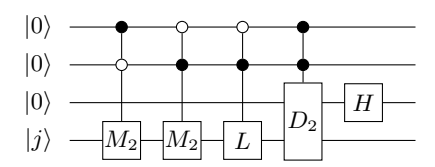


**Figure 13.** The quantum circuit for the  $O_c$  oracle associated with an extended binary tree.

## **4.2.2** The $O_A$ circuit

As we indicated earlier, the construction of the  $O_A$  quantum circuit depends closely on how  $O_C$  is contructed. For the adjacency matrix associated with the extended binary tree, the  $O_A$  circuit corresponding to the  $O_C$  circuit shown in fig. 13 can be constructed as follows.

- 1. First, we use a rotation of angle  $\theta_1 = \arccos(\alpha) 1$  controlled by  $\ell = 0$  to place  $\alpha$  on the diagonal of the principal leading block of  $U_A$ .
- 2. We then use a rotation of angle  $\theta_2 = \arccos(\beta)$  controlled by  $\ell = 1$  to place  $\beta$  at  $U_{A_{i,j}}$  for i = 2j,  $0 \le i, j \le N 1$ .
- 3. Similarly, we use a rotation of angle  $\theta_2$  controlled by  $\ell=2$  to place  $\beta$  at  $U_{A_{i,j}}$  for  $i=2j+1, 0 \leq i, j \leq N-1$ .
- 4. We then need to zero out  $U_{A_{i,j}}$  for leaf vertices j using a rotation of angle  $\theta_3 = \pi/2 \theta_2$  controlled by both  $\ell = 1, 2$  and  $4 \le j \le N$ .
- 5. We then need to adjust the diagonal elements associated with the leaf vertices and the root vertex by applying a rotation of angle  $\theta_4 = \arccos(\gamma) \theta_1$  controlled by j = 0 or  $0 \le j \le N 1$  and  $\ell = 0$ .
- 6. Finally, to place  $\beta$  at  $U_{Ai,j}$  for  $i = \lfloor j/2 \rfloor$ , we need to apply a rotation of angle  $\theta_5 = \arccos(\beta)$  controlled by  $\ell = 3$

The complete  $O_A$  circuit resulting from the above procedure can be drawn as shown in fig. 14.

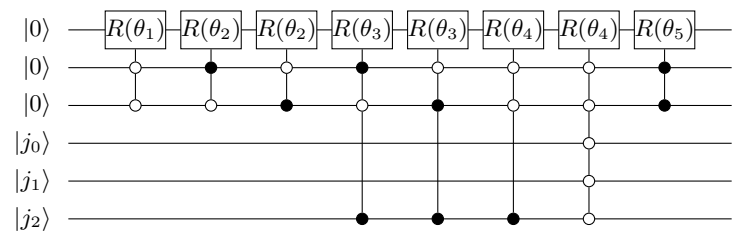


**Figure 14.** The  $O_A$  quantum circuit for the adjacency matrix associated with an extended binary tree shown in eq. (4.21).

## 4.2.3 The complete circuit

Combining the  $O_C$  and  $O_A$  circuits, we obtain the complete circuit for the block encoding of the  $8 \times 8$  adjacency matrix associated with the 8-vertex extended binary tree as shown in fig. 15.

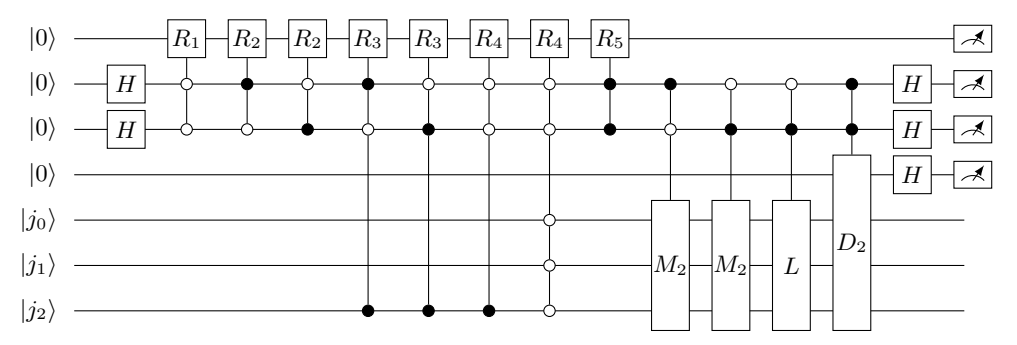


**Figure 15.** The full quantum circuit for the adjacency matrix associated with an extended binary tree shown in eq. (4.21).

This circuit can be easily generalized for larger adjacency matrices associated with an extended binary tree with a larger number  $(N=2^n)$  of vertices. However, because the number of unique cases defined by the function  $c(j,\ell)$  in (4.22) is a constant 4 due to the relatively small number of additional vertices each vertex is connected to, the number of the controlled multiplication, division and additional gates in  $O_C$  is fixed. Furthermore, because the number of distinct values of matrix elements in A is fixed at 3, the number of controlled rotations required in  $O_A$  is also fixed. Each of these controlled rotations can be further decomposed into a subcircuit with  $\mathcal{O}(\text{poly}(n))$  two-qubit gates. The overall gate complexity of the quantum circuit is  $\mathcal{O}(\text{poly}(n))$ , which is considered efficient.

## 4.3 Hermitian block encoding of Hermitian sparse matrices

In general, the block encoding unitary of a real symmetric or complex Hermitian matrix is not necessarily symmetric or Hermitian. This is clearly the case for the block encodings constructed in sections 4.1 and 4.2. It is also possible to obtain a Hermitian block encoding of a Hermitian matrix, which can simplify certain theoretical treatments (e.g. quantum walks). We will show how an efficient quantum circuit can be constructed for such a block encoding. The following theorem lays out the basic structure of such a circuit, which can be viewed as a variant of Szegedy's quantum walk construction in Szegedy [2004], Childs [2010].

**Theorem 4.2.** Suppose A is a sparse Hermitian matrix with at most s non-zeros per column, and  $s = 2^m$ . If a unitary  $O_C$  satisfies

$$O_C |\ell\rangle |j\rangle = |c(j,\ell)\rangle |j\rangle,$$
 (4.23)

where  $c(j,\ell)$  is the row index of the  $\ell$ th non-zero elements in the jth column, and if there exists a unitary  $O_A$  such that

$$(I \otimes O_A) |0\rangle |0\rangle |i\rangle |j\rangle = |0\rangle \left(\sqrt{A_{ij}} |0\rangle + \sqrt{1 - |A_{ij}|} |1\rangle\right) |i\rangle |j\rangle, \qquad (4.24)$$

then the unitary  $U_A$  represented by the circuit shown in fig. 16 is a Hermitian block encoding of A, where  $D_s$  is a diffusion operator applied to n qubits as

$$D_s |0^n\rangle = \frac{1}{\sqrt{s}} \sum_{\ell=0}^{s-1} |\ell\rangle,$$

and SWAP is a swap operator that swaps the first two qubits as well as the last two n-qubit registers in fig. 16 respectively.

**Figure 16.** The general structure of a quantum circuit for a Hermitian block encoding of an s-sparse Hermitian matrix A. The S block represents a SWAP operator that swaps the the last two n-qubit registers qubit-by-qubit.

*Proof.* Our goal is to show that  $\langle 0|\langle 0^m|\langle i|U_A|0\rangle|0^m\rangle|j\rangle=A_{ij}/s$ . In order to compute the inner product  $\langle 0|\langle 0^m|\langle i|U_A|0\rangle|0^m\rangle|j\rangle$ , we apply  $D_s,O_A,O_c$  to  $|0\rangle|0^m\rangle|j\rangle$  successively as illustrated below

$$|0\rangle |0^{m}\rangle |j\rangle \xrightarrow{D_{s}} \frac{1}{\sqrt{s}} \sum_{\ell \in [s]} |0\rangle |\ell\rangle |j\rangle$$

$$\xrightarrow{O_{A}} \frac{1}{\sqrt{s}} \sum_{\ell \in [s]} \left( A_{c(j,\ell),j} |0\rangle + \sqrt{1 - |A_{c(j,\ell),j}|^{2}} |1\rangle \right) |\ell\rangle |j\rangle$$

$$\xrightarrow{O_{c}} \frac{1}{\sqrt{s}} \sum_{\ell \in [s]} \left( A_{c(j,\ell),j} |0\rangle + \sqrt{1 - |A_{c(j,\ell),j}|^{2}} |1\rangle \right) |\ell\rangle |c(j,\ell)\rangle.$$

$$(4.25)$$

Instead of multiplying the last factor  $I_2 \otimes D_s \otimes I_n$  in (4.4) to the last line of (4.25), we apply it to  $|0\rangle |0^m\rangle |i\rangle$  first to obtain

$$|0\rangle |0^{m}\rangle |i\rangle \xrightarrow{D_{s}} \frac{1}{\sqrt{s}} \sum_{\ell' \in [s]} |0\rangle |\ell'\rangle |i\rangle.$$
 (4.26)

Finally, taking the inner product between (4.25) and (4.26) yields

$$\langle 0 | \langle 0^m | \langle i | U_A | 0 \rangle | 0^m \rangle | j \rangle = \frac{1}{s} \sum_{\ell} A_{c(j,\ell),j} \delta_{i,c(j,\ell)} = \frac{1}{s} A_{ij}.$$
 (4.27)

We use the  $8 \times 8$  banded circulant matrix defined by (4.9) with  $\beta = \gamma$  as an example to illustrate how to construct an efficient quantum circuit for a Hermitian block encoding of a Hermitian sparse matrix.

For this example, we define  $c(j,\ell)$  to be used in the construction of the  $O_C$  circuit as

$$c(j,\ell) = \ell + j - 1,$$
 (4.28)

to represent the row index of the  $\ell$ th non-zero matrix elements in the jth column. It is important to notice that the definition of  $O_C$  in (4.23) is different from the definition given in (4.2). In (4.2), the qubit register that takes  $|j\rangle$  as the input is changed and the register used to hold  $|\ell\rangle$  is simply used as a control and is not altered after the unitary transformation. In (4.23), the register that holds  $|\ell\rangle$  is changed while  $|j\rangle$  is unchanged. Therefore, we need to construct a circuit that adds j-1 to  $\ell$  using  $|j\rangle$  as the control. The addition of j to a quantum state can be represented by  $L^j$  controlled by  $|j\rangle$ .

Let  $j = [\mathbf{j}_0 \mathbf{j}_1 \cdots \mathbf{j}_{n-2} \mathbf{j}_{n-1}] = \mathbf{j}_0 \cdot 2^{n-1} + \mathbf{j}_1 \cdot 2^{n-2} + \cdots + \mathbf{j}_{n-2} \cdot 2^1 + \mathbf{j}_{n-1} \cdot 2^0$  be the binary representation of the integer  $j \in \mathbb{N} : 0 \le j \le 2^n - 1$ , where  $j_k \in \{0,1\}$  for  $0 \le k \le n-1$ . Substituting this binary representation of j into  $L^j$  yields

$$L_n^j = \left(L_n^{2^{n-1}}\right)^{j_1} \cdot \left(L_n^{2^{n-2}}\right)^{j_2} \cdots \left(L_n^{2^0}\right)^{j_n}. \tag{4.29}$$

As we have already seen in (4.12) that an n-qubit L-shift operator satisfies

$$L_n^2 = L_{n-1} \otimes I_2.$$

As a result, we may use the circuit shown in fig. 17 to map  $|\ell\rangle |j\rangle$  to  $|c(j,\ell)\rangle |j\rangle$ .

The construction of the  $O_A$  circuit in this example is similar to the way  $O_A$  is constructed in section 4.1. We use rotations controlled by  $\ell$  to place non-zero  $\sqrt{A_{ij}}$  at appropriate locations in the principal leading block of  $U_A$ . To

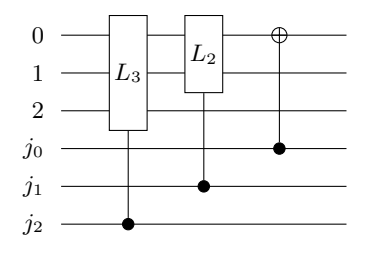


**Figure 17.** A quantum circuit for  $L_3^j$ .

be specific, we use the rotation  $R(\theta_1)$  with the angle  $\theta_1 = \arccos(\sqrt{\beta} - 1)$  conditioned on  $\ell = 0$  to place  $\beta$  on the supdiagonal. We use the rotation  $R(\theta_2)$  with  $\theta_2 = \arccos(\sqrt{\alpha}) + \pi$  conditioned on  $\ell = 1$  to place  $\alpha$  on the diagonal, and the rotation  $R(\theta_3)$  with  $\theta_3 = \arccos(\beta) + \pi$  to place  $\beta$  on the subdiagonal.

The complete circuit for the Hermitian block encoding of A is shown in fig. 18.

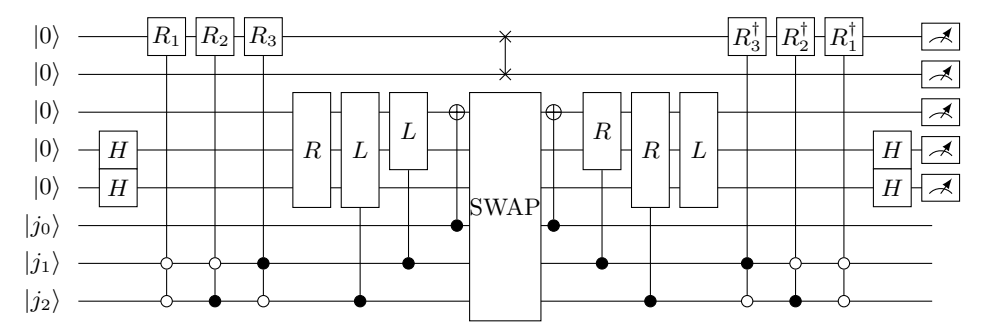


**Figure 18.** The complete quantum circuit for a Hermitian block encoding of the  $8 \times 8$  Hermitian banded circulant matrix A defined by (4.9). The SWAP operator swaps the last two n-qubit registers qubit-by-qubit.

#### 5 Efficient circuits for quantum walks

In this section, we examine efficient quantum circuits for the block encoding of a special type of sparse matrices P, called a Markov chain matrix or a stochastic matrix. This type of matrix represents the transition probabilities of traversing from one vertex to another in a random walk on a graph G = (V, E). Since the matrix element  $P_{ij}$  represents the probability of walking from vertex i to vertex j, it satisfies

$$P_{ij} \ge 0, \quad \sum_{i} P_{ij} = 1.$$
 (5.1)

A stochastic matrix has many interesting properties, which are briefly summarized in the appendix. In particular, it can be used to model a classical random walk, which is described by  $w = P^k v$ , where the *i*th element of the initial state v specifies the probability of a walker being at vertex i initially, and the *i*th element of the final state w gives the probability of the walker being at vertex i after k steps of random walks have been taken using P as the transition probability. The efficiency of the walk is often measured in terms of the number of steps it takes to reach a certain vertex (hitting time).

For a symmetric P, which is also called a doubly stochastic Markov chain matrix, and is what we consider later in this section, a more efficient type of walk, called *quantum walk* Mackay et al. [2002], Venegas-Andraca [2012] can be constructed by block encoding  $T_k(P)$ , where  $T_k(t) = \cos(k \arccos(t))$  is the kth degree Chebyshev polynomial of the first kind. When such a block encoding is applied to an initial state prepared as  $v \otimes |0\rangle$ , it yields

$$w = |T_k(P)v\rangle \otimes |0\rangle + |*\rangle |1\rangle, \tag{5.2}$$

where \* denotes a vector that we do not care about. After measuring the second register and obtaining  $|0\rangle$ , the first register contains  $|T_k(P)v\rangle$ . This suggests that performing k steps of a quantum walk yields  $T_k(P)v$  instead of  $P^kv$ . The consequence such a transformation will be discussed in the appendix through a specific application of a quantum

walk. Quantum walks have found many other applications in quantum algorithms Shenvi et al. [2003], Paparo and M. [2012].

In this section, we discuss efficient quantum circuits for the block encoding of  $T_k(P)$ , which is in turn expressed in terms of the block encoding of P.

## 5.1 Direct block encoding of P and $T_k(P)$

For an s-sparse P, we can use the techniques discussed in section 4 to construct an efficient quantum circuit that block encodes P/s. In particular, if P is symmetric, we can construct a symmetric block encoding of P/s.

Once we have the block encoding for P/s, we can use the QET discussed in section 3 to construct a quantum circuit for a block encoding of  $T_k(P/s)$ . However, our ultimate goal for implementing a quantum walk is not to have a block encoding of  $T_k(P/s)$  but  $T_k(P)$  because P/s is not a stochastic matrix corresponding to a random walk.

To overcome this difficulty, we may express the kth degree Chebyshev polynomial  $T_k(t)$  in terms of  $T_j(t/s)$  for j = 0, 1, ..., k, i.e.,

$$T_k(t) = \tilde{T}_k(t') = \sum_{j=0}^k \alpha_j T_j(t'),$$
 (5.3)

where t' = t/s and  $\alpha_j = 0$  for odd (even) j if k is even (odd).

For example, when s = 4,

$$T_2(t) = \tilde{T}_2(t') = 15 + 16T_2(t'), \text{ where } t' = t/4.$$
 (5.4)

We then try to use the QET to construct a block encoding of  $\tilde{T}_k(t')$ . However, to use the QET, the magnitude of the polynomial  $\tilde{T}_k(t')$  must be bounded by 1 within the interval [-1,1]. Since the magnitude of  $\tilde{T}_k(t')$  can be much larger than 1 at  $t'=\pm 1$ , we need to scale  $\tilde{T}_k(t')$  by  $1/|\tilde{T}_k(1)|$  before using the QET. For example, for s=4,  $\tilde{T}_2(1)=31$ . As a result, we need to divide  $\tilde{T}_2(t')$  in (5.4) by 31 before applying the QET. Consequently, we effectively construct a block encoding for  $T_k(P)/\alpha$ , where  $\alpha=\tilde{T}_k(1)$ , instead of  $T_k(P)$ . This has the effect of lowering the probability of successful measurement of  $|0\rangle$  in (5.2) (when  $T_k(P)$  is replaced with  $T_k(P)/\alpha$ .)

Nonetheless, we can construct a quantum circuit for such a block encoding. For k = 2, it follows from the discussion in section 3 and fig. 2 that such a circuit can be drawn as the one shown in fig. 19, where the phase angles

$$\phi_0 = 1.17, \ \phi_1 = 0.8, \ \phi_2 = 1.17$$

can be found numerically by using the QSPPACK Dong et al. [2021] software and  $U_{P/s}$  denotes the block encoding of P/s.

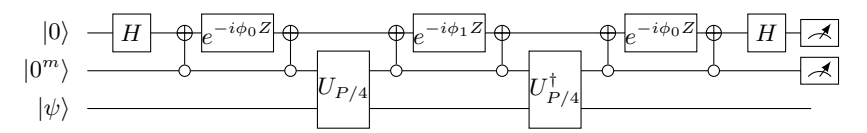


**Figure 19.** A quantum circuit for  $T_2(P)/31$  for a sparse symmetric stochastic matrix P with at most 4 nonzero matrix elements per column using  $U_{P/4}$  which is the block encoding for P/4.

#### 5.2 Szegedy's quantum walk

There is a way to block encode P instead of P/s. Such a block encoding scheme relies on using a different unitary oracle  $O_P$  that carries out the following mapping

$$O_P |0^n\rangle |j\rangle = \sum_k \sqrt{P_{jk}} |k\rangle |j\rangle.$$
 (5.5)

Thanks to the stochasticity of P, the right hand side is already a normalized vector, and no additional ancilla qubit is needed.

The following theorem describes the structure of the blocking encoding constructed from a combination of  $O_P$  and an n-qubit swap operator that performs the following operation

SWAP 
$$|i\rangle |j\rangle = |j\rangle |i\rangle$$
, (5.6)

which swaps the value of the two registers in the computational basis, and can be directly implemented using n two-qubit SWAP gates.

**Theorem 5.1.** If P is a doubly stochastic Markov chain matrix, and if there exists a unitary operator  $O_P$  that can be used to carry out the mapping defined in Eq. (5.5), then

$$U_P = O_P^{\dagger} \, \text{SWAP} \, O_P \tag{5.7}$$

is a Hermitian block encoding of P, where the swap operator SWAP is defined by Eq. (5.7).

*Proof.* Clearly  $U_P$  is unitary and Hermitian. Now we compute as before

$$|0^{n}\rangle|j\rangle \xrightarrow{O_{P}} \sum_{k} \sqrt{P_{jk}}|k\rangle|j\rangle \xrightarrow{\text{SWAP}} \sum_{k} \sqrt{P_{jk}}|j\rangle|k\rangle.$$
 (5.8)

Meanwhile

$$|0^{n}\rangle|i\rangle \xrightarrow{O_{P}} \sum_{k'} \sqrt{P_{ik'}}|k'\rangle|i\rangle.$$
 (5.9)

The inner product of (5.8) and (5.9) yields (using  $P_{ij} = P_{ji}$ )

$$\langle 0^n | \langle i | U_P | 0^n \rangle | j \rangle = \sum_{k,k'} \sqrt{P_{ik'} P_{jk}} \delta_{j,k'} \delta_{i,k} = \sum_{k,k'} \sqrt{P_{ij} P_{ji}} = P_{ij}.$$
 (5.10)

Note the doubly stochastic requirement for P in the above theorem is not essential. When  $P \neq P^T$ , we can work with the discriminant matrix defined in the appendix. To simplify notation, we assume P is doubly stochastic below.

We now discuss how to construct an efficient circuit for  $O_P$  using the banded circulant matrix (4.9) as an example, where we assume  $\alpha + \beta + \gamma = 1$  for the matrix to be stochastic. The construction of a block-encoding circuit can be done in two steps. In the first step, we construct a unitary K to perform the following mapping

$$K|0^{n}\rangle = (\sqrt{\alpha}\sqrt{\beta}\,0\,\cdots\,0\,\sqrt{\gamma})^{T}.\tag{5.11}$$

The first column of K has to encode the square root of the first column of the circulant matrix. It is generally possible to construct a circuit for performing such a unitary transformation using a method proposed in Vartiainen et al. [2004]. The method uses Gray code ordering and fully-controlled quantum Givens rotations to construct the circuit. Our approach is similar, but exploits the sparsity of the vector v to reduce the gate complexity to  $\mathcal{O}(n)$  for this special case. We use a sequence of (multi-qubit controlled) CNOTs shown in fig. 20 to permute the non-zero element in the N-1st row to row 3. We can now zero out  $\sqrt{\gamma}$  in row 3 by applying the rotation  $R(\theta_2)$  with  $\theta_2 = -\arctan\sqrt{\frac{\gamma}{\beta}}$  to the row 1 and 3 of resulting state. Finally, we can zero out the element  $\sqrt{\beta+\gamma}$  in row 1 of the resulting state against  $\sqrt{\alpha}$  in row 0 with the rotation  $R(\theta_1)$  where  $\theta_1 = -\arctan\sqrt{\frac{\beta+\gamma}{\alpha}}$ . This rotation is applied to rows 0 and 1 of the state. To obtain a circuit for K, we reverse the order of operations listed above and negate the signs on the rotation angles as shown in Figure 20.

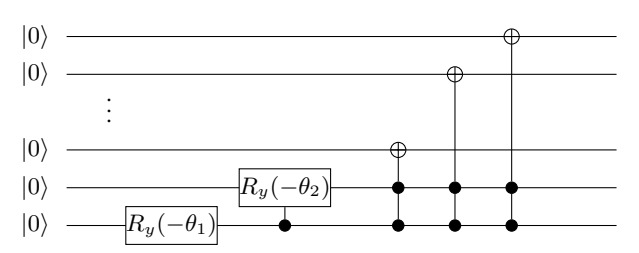


**Figure 20.** A quantum circuit for the state preparation unitary K given in (5.11).

In the second step, we use the fact that  $Pe_j = L_n^{j-1}Pe_1$ , where  $e_j$  is the jth column of the identity matrix, to construct a controlled shift (adder) circuit to map  $|Pe_1\rangle|j\rangle$  to  $|Pe_j\rangle|j\rangle$ . This is the same controlled L-shift circuit we constructed in section 4.3 to implement the mapping (4.23). Combining these two steps as well as the SWAP operator, we can represent the quantum circuit for the Hermitian block encoding of P by the diagram shown in fig. 21.

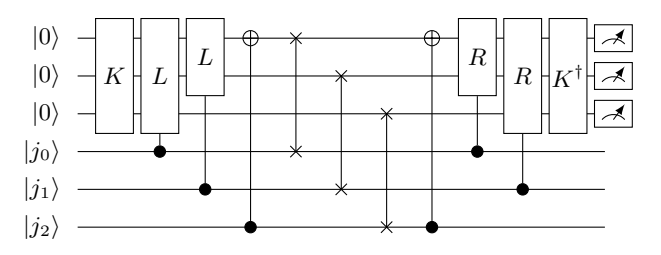


**Figure 21.** The complete quantum circuit for a Hermitian block encoding of the  $8 \times 8$  Hermitian banded circulant matrix P defined by (4.9) with  $\alpha > 0$ ,  $\gamma = \beta > 0$  and  $\alpha + 2\beta = 1.0$ .

Once a quantum circuit for a symmetric block encoding of P is available, we can then use QET to construct a circuit that block encodes  $T_k(P)$  for a kth degree of Chebyshev polynomial. It can be easily shown that the phase angles required in the QET circuit are

$$\varphi_0 = \pi/2, \ \varphi_1 = \dots = \varphi_{k-1} = \pi/2 \text{ and } \varphi_k = 0.$$
 (5.12)

It follows from the discussion in section 3 that the circuit for the block encoding of  $T_k(P)$  has a structure shown in fig. 22.

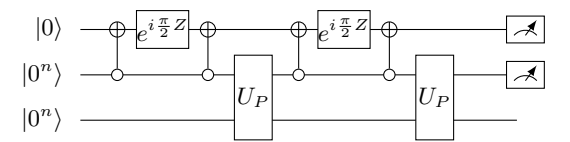


**Figure 22.** The overall structure of a quantum circuit for the block encoding of  $T_2(P)$ .

Note that the first two multi-qubit controlled NOT gates and the single qubit phase gate labelled by  $e^{i\frac{\pi}{2}Z}$  are used to implement the  $e^{i\frac{\pi}{2}Z_{\Pi}}$  operator, where  $Z_{\Pi}$  is a reflector defined as

$$Z_{\Pi} \equiv 2\Pi - I,$$

with  $\Pi \equiv |0^n\rangle \langle 0^n| \otimes I_N$ . In general, such a circuit block is used to implement  $e^{i\phi Z_\Pi}$ , which appears in the block encoding of a matrix polynomial, for an arbitrary angle  $\phi$ . However, when  $\phi = \pi/2$ , we can use the fact that  $e^{i\frac{\pi}{2}Z_\Pi} = -iZ_\Pi$  to simplify the block encoding circuit. We can rewrite the block encoding of  $T_k(P)$  simply as (up to an irrelevant global phase factor  $(-i)^k$ )

$$U_{T_k(P)} = (U_P Z_{\Pi})^k \,. \tag{5.13}$$

Substituting the symmetric block encoding  $U_P$  defined in (5.7) into (5.13) and grouping  $O_P^{\dagger}$ ,  $Z_{\Pi} \otimes I$ ,  $O_P$  and SWAP together allows us to express  $U_{T_k(P)}$  in terms of repeated application of

$$SWAP \cdot U_R, \tag{5.14}$$

where  $U_R \equiv O_P (Z_\Pi \otimes I) O_P^{\dagger}$ . This indicates that the block encoding of  $T_k(P)$  is equivalent to performing k steps of a Szegedy quantum walk, which is typically defined as the product of a reflection and a swap operator. We will show this equivalence more precisely in the Appendix.

It follows that constructing an efficient circuit for the Szegedy quantum walk is equivalent to constructing an efficient circuit for the symmetric block encoding of P defined in (5.7). We should note that a method for constructing efficient quantum circuits for a Szegedy quantum walk on structured graphs was previously presented in Loke and Wang [2017]. We now show that this method is equivalent to the construction of the block encoding circuit for P.

The method presented in Loke and Wang [2017] seeks a unitary transformation V in the form of  $\sum_{i=0}^{N-1} V_i \otimes |i\rangle \langle i|$  to diagonalize  $U_R$ . If  $V_i$ 's can be found to satisfy  $V_i |\phi_i\rangle = |b\rangle$  for a computational basis  $|b\rangle$ , then one can verify that

$$V^{\dagger}U_{R}V = 2\sum_{i=0}^{N-1} \left(V_{i}^{\dagger} |\phi_{i}\rangle \langle \phi_{i}| V_{i}\right) \otimes |i\rangle \langle i| = 2(|b\rangle \langle b| - I). \tag{5.15}$$

If  $|b\rangle$  is chosen to be  $|0^n\rangle$ , the right hand side of (5.15) becomes the  $Z_{\Pi}$  matrix appeared in (5.13).

The transformation V defined in (5.15) is equivalent to the  $O_P$  transformation defined by (5.5). Hence, constructing a circuit for  $O_P$  is equivalent to constructing a circuit for V. When this circuit is combined with the circuit implementation of  $Z_{\Pi}$ , we obtain a quantum circuit for the Szegedy quantum walk that is equivalent to the construction of an efficient circuit for the block encoding of P given by (5.7).

# 6 Concluding remarks

We discussed techniques for constructing an efficient quantum circuit for the block encoding of an s-sparse matrix A/s and gave some specific examples. In general, the block encoding circuit consists of an  $O_c$  circuit block that encodes the nonzero structure of the matrix and an  $O_A$  circuit that encodes the numerical values of the nonzero matrix elements. Without an efficient implementation of these oracles with poly(n) gate complexity, it can be very difficult to achieve exponential quantum advantage over classical algorithms Tang [2021], Gharibian and Gall [2021]. Through explicit examples, we show that the construction of these circuit blocks may not be completely independent of each other. In particular, the  $O_A$  circuit may be constructed to zero out certain matrix element to maintain the desired sparsity structure.

For a general sparse matrix A, constructing an efficient block encoding of A/s can be non-trivial. In particular, it may be difficult to find an efficient  $O_c$  if the sparsity pattern of A is somewhat arbitrary. In some cases, a more general block encoding scheme that includes an additional  $O_r$  unitary that encodes the row sparsity separately from the column sparsity may be needed.

The general construction procedure is not suitable for block encoding a sparse doubly stochastic matrix P associated with a random walk on a graph when such a block encoding is used to implement a quantum walk on the same graph. For this type of matrices, an alternative construction procedure that yields a symmetric block encoding circuit for P instead of P/s is desired. Such a block encoding allows us to construct a block encoding of a Chebyshev polynomial of P, which is the unitary used in a quantum walk. We showed that constructing a circuit for a block encoding of P is equivalent to a previously developed technique for constructing an efficient quantum circuit for Szegedy quantum walks on special graphs.

Throughout this paper, we assume that single qubit gates are available for an arbitrary rotation matrix, and that multiqubit controls are available to carry out the required encoding schemes. No constraint has been placed on the topology of qubits and their connections. This is certainly not the case for existing quantum devices, and these assumptions are not expected to be valid at least for early fault-tolerant quantum computers. When the quantum gates available on these devices are restricted to a few elementary gates (such as Hadamard and Pauli gates), additional decompositions and transformations are required to express some of the gates (especially, the multi-qubit control gates) used in the block encoding circuits described above in terms of elementary gates. The circuit construction will also need to take the topology and connection of qubits into consideration. We will pursue efficient ways to construct this type of circuits in future works.

## **Acknowledgments:**

This work was partially supported by the Department of Energy (DOE) under Contract No. DE-AC02-05CH11231 and DE-SC0017867, through the Quantum Systems Accelerator program (L.L., C.Y.), the DOE Office of Advanced Scientific Computing Research (ASCR) Accelerated Research for Quantum Computing Program (C.Y.), and the Laboratory Directed Research and Development Program of Lawrence Berkeley National Laboratory (R. VB and D. C.). L.L. is a Simons Investigator.

# 7 Appendix

In this section, we provide additional materials that describe properties of a random walk as well as an application that demonstrates the higher (query) efficiency of a quantum walk compared to that of a classical random walk.

#### 7.1 Properties a Markov chain matrix

Because the sum of all probabilities of transitions from the vertex i to other vertices must be 1 for all i, the vector  $(1 \ 1 \cdots 1)^T$  is a right eigenvector of the Markov chain stochastic matrix P associated with the eigenvalue 1. The

corresponding left eigenvector  $\pi$  is called a *stationary state* and satisifies

$$\pi^T P = \pi, \quad \pi_i \ge 0, \quad \sum_i \pi_i = 1.$$
 (7.1)

A Markov chain matrix P is *irreducible* if any state can be reached from any other state in a finite number of steps of a random walk, i.e., the jth element of  $w = P^k e_i$  is nonzero for any j and some finite k where  $e_i$  is the ith column of the identity matrix. An irreducible Markov chain is *aperiodic* if there exists no integer greater than one that divides the length of every directed cycle of the graph. A Markov chain is ergodic if it is both irreducible and aperiodic. By the Perron–Frobenius Theorem, any ergodic Markov chain P has a unique stationary state  $\pi$  in (7.1). A Markov chain is ergodic if the following detailed balance condition is satisfied

$$\pi_i P_{ij} = \pi_j P_{ji}. \tag{7.2}$$

For a nonsymmetric but reversible P, we can construct a quantum walk by block encoding the discriminant matrix D associated with P. Such a matrix is defined componentwise as

$$D_{ij} = \sqrt{P_{ij}P_{ii}},\tag{7.3}$$

which is real symmetric.

When P is reversible, it can be shown that

$$|\pi\rangle = \sum_{i} \sqrt{\pi_i} |i\rangle \tag{7.4}$$

is a normalized eigenvector of the discrimant matrix D defined by (7.3), i.e.,  $|\pi\rangle$  satisfies

$$D\left|\pi\right\rangle = \left|\pi\right\rangle. \tag{7.5}$$

Furthermore, because  $\pi_i > 0$  for all i, we have

$$D = \operatorname{diag}(\sqrt{\pi}) P \operatorname{diag}(\sqrt{\pi})^{-1}. \tag{7.6}$$

Therefore, for a reversible P, P and D share the same set of eigenvalues, and the spectral properties of a nonsymmetric P can be analyzed by working with the symmetric D matrix.

## 7.2 The equivalence of Szegedy quantum walk and block encoding of $T_k(D)$

The Szegedy quantum walk can also be presented as follows. Using the  $O_P$  oracle and the multi-qubit SWAP gate, we can define two set of quantum states

$$|\psi_{j}^{1}\rangle = O_{P} |0^{n}\rangle |j\rangle = \sum_{k} \sqrt{P_{jk}} |k\rangle |j\rangle,$$

$$|\psi_{j}^{2}\rangle = \text{SWAP}(O_{P} |0^{n}\rangle |j\rangle) = \sum_{k} \sqrt{P_{jk}} |j\rangle |k\rangle.$$
(7.7)

This defines two projection operators

$$\Pi_{l} = \sum_{j \in [N]} |\psi_{j}^{l}\rangle \langle \psi_{j}^{l}|, \quad l = 1, 2,$$

$$(7.8)$$

from which we can define two 2n-qubit reflection operators  $R_{\Pi_l} = 2\Pi_l - I_{2n}$ . Let us write down the reflection operators more explicitly. Using the resolution of identity,

$$R_{\Pi_1} = O_P((2|0^n) \langle 0^n | - I) \otimes I_n) O_P^{\dagger} = O_P(Z_{\Pi} \otimes I_n) O_P^{\dagger}. \tag{7.9}$$

Similarly

$$R_{\Pi_2} = \text{SWAP } O_P(Z_{\Pi} \otimes I_n) O_P^{\dagger} \text{ SWAP}.$$
 (7.10)

Then Szegedy's quantum walk operator takes the form

$$\mathcal{U}_Z = R_{\Pi_2} R_{\Pi_1},\tag{7.11}$$

which is a rotation operator that resembles Grover's algorithm. Note that

$$\mathcal{U}_{Z} = \text{SWAP } O_{P}(Z_{\Pi} \otimes I_{n}) O_{P}^{\dagger} \text{SWAP } O_{P}(Z_{\Pi} \otimes I_{n}) O_{P}^{\dagger}, \tag{7.12}$$

so  $O_P^{\dagger} \mathcal{U}_Z(O_P^{\dagger})^{-1}$  is the same as a block encoding of  $T_2(D)$  using qubitization up to a matrix similarity transformation. More generally, k-steps of Szegedy's quantum walk given by  $\mathcal{U}_Z^k$  is equivalent to a block encoding of  $T_{2k}(D)$ .

#### 7.3 Quantum walk application: detecting a marked vertex

In this section, we provide a brief explanation of the advantage of a quantum walk over a classical random walk, i.e., why it is of interest to block encode  $T_k(D)$  and perform the corresponding unitary transformation (5.2) on a quantum computer rather than simply applying  $P^k$  to an initial vector of probability distributions on a classical computer.

The direct consequence of applying  $T_k(P)$  in a quantum walk (instead of  $P^k$  in a classical random walk) to v can be analyzed as follows. Since an eigenvalue  $\lambda$  of P is between -1 and 1, we can reparameterize it as  $\lambda = \cos \theta$ . Clearly, the corresponding eigenvalue of  $P^k$  is  $\cos^k \theta$ , and the corresponding eigenvalue of  $T_k(P)$  is  $\cos(k\theta)$ . For small  $\theta$ , it follows from the Taylor expansion of  $\cos^k \theta$  and  $\cos \hat{k}\theta$  that

$$\cos^k \theta = 1 - \frac{k\theta^2}{2} + O(k^2 \theta^4), \tag{7.13}$$

$$\cos \hat{k}\theta = 1 - \frac{\hat{k}^2 \theta^2}{2} + O(\hat{k}^4 \theta^4), \tag{7.14}$$

for integers k and  $\hat{k}$ .

We can readily see that the Taylor expansions of these functions agree up to the second order term when  $\hat{k} = \sqrt{k}$ . This observation suggests that, for a reversible random walk, the second largest eigenvalue of  $T_{\hat{k}}(P)$  can reach that of  $P^k$  when  $\hat{k} = O(\sqrt{k})$ . Since properties of a random walk is often determined by the gap between the largest eigenvalue and the second largest eigenvalue, this observation highlights the fundamental reason why a quantum walk can be asymptotically much faster than a classical random walk.

To demonstrate how a quantum walk can be used to solve a practical problem, let us examine the following example. Our goal is to detect the presence of a marked vertex in a graph G=(V,E). Our assumption is that we do not know a priori whether such a marked vertex exists. Nor do we know the location of this vertex if it indeed exists. What we are given are some tools we can use to find out the presence of the marked vertex and its position if it is present.

In the classical setting, the tool we are given is a random walk transition probability matrix P (constructed by someone who knows the answer). We are allowed to apply P to a vector and check the result (but not allowed to look at P itself). The vector we will apply P to is prepared as v = e/N, where  $e = (1, \ldots, 1)^T$ . It describes an intial uniform probability of being at any vertex. We examine the probability of being at each vertex after performing several steps of the random walk, i.e., we examine elements of the vector  $w = P^k v$ . If G contains a marked vertex, the element of w associated with such vertex will have a much higher magnitude. The position of this element informs us the position of the marked vertex.

If no marked vertex is present in G, the matrix P we are given is

$$P = \frac{1}{N} e e^{\top}, \quad e = (1, \dots, 1)^{\top}.$$
 (7.15)

Otherwise, if a marked vertex is present, and if, without loss of generality, the marked vertex is the 0-th vertex (which we do not know in advance), the matrix P we are given is

$$P = \begin{pmatrix} 1 & 0\\ \frac{1}{N}\widetilde{e} & \frac{1}{N}\widetilde{e}\widetilde{e}^{\top} \end{pmatrix}, \tag{7.16}$$

where  $\tilde{e}$  is a vector of all ones of length N-1.

Clearly, applying the P matrix defined by (7.15) to v does not change v. The output from such a random walk remains the same, i.e., the probability of being at each vertex remains at 1/N.

However, if we are given the P matrix defined by (7.16), one can show that  $w = P^k v$  converges to the eigenvector  $\widetilde{\pi} = (1, 0, \dots, 0)^{\mathsf{T}}$  associated with the largest eigenvalue 1 of P when  $k = \mathcal{O}(N)$ . Hence, after performing  $\mathcal{O}(N)$  steps of the random walk using this P, we can conclude, with high confidence, that there is a marked vertex and it is the 0th vertex since the 0th element of w is nearly 1.

In the quantum setting, the tool we are given is different. Instead of the P matrix, we are given the block encoding of the discriminant matrix D associated with P denoted by  $U_D$ . Again, we are allowed to apply  $U_D^k$  to a carefully prepared quantum state  $|\psi_0\rangle$  to perform a quantum walk (but not allowed to look at  $U_D$  itself). The prepared initial quantum state is

$$|\psi_0\rangle = |0^n\rangle (H^{\otimes n} |0^n\rangle). \tag{7.17}$$

To acertain the presence of a marked vertex, which is equivalent to determining whether the quantum walk operator is the block encoding of the discriminant matrix associated with the P matrix defined in (7.15) or (7.16), we measure the first n qubits, and evaluate the success probability of measuring the  $|0^n\rangle$  state. This probability should be

$$p(|0^n\rangle) = \|(|0^n\rangle\langle 0^n| \otimes I_n)U_D^k |\psi_0\rangle\|^2. \tag{7.18}$$

Then if  $U_D$  were the block encoding of P (which is the same as the corresponding discriminant matrix D when  $P = P^T$ ),  $U_D |\psi_0\rangle = |\psi_0\rangle$ . As a result, the probability of measuring  $|0^n\rangle$  is  $p(|0^n\rangle) = 1$ , regardless how many steps of the quantum walk are taken.

On the other hand, if  $U_D$  results from the block encoding of the discriminant matrix D associated with the P matrix defined in (7.16), which has the form

$$D = \begin{pmatrix} 1 & 0 \\ 0 & \frac{1}{N}\widetilde{e}\widetilde{e}^{\top} \end{pmatrix}, \tag{7.19}$$

the success probability of measuring  $|0^n\rangle$  can be much less than 1.

To see this, we recognize that the matrix D defined in (7.19) has two nonzero eigenvalues 1 and  $(N-1)/N=1-\delta$ , with the corresponding eigenvectors  $|\widetilde{\pi}\rangle=(1,0,...,0)^{\top}$  and  $|\widetilde{v}\rangle=\frac{1}{\sqrt{N-1}}(0,1,1\ldots,1)^{\top}$ , respectively. Because

$$|\psi_0\rangle = \frac{1}{\sqrt{N}} |0^n\rangle |\widetilde{\pi}\rangle + \sqrt{\frac{N-1}{N}} |0^n\rangle |\widetilde{v}\rangle, \qquad (7.20)$$

it follows from the fact that  $U_D^k$  block encodes  $T_k(D)$  that

$$U_D^k |\psi_0\rangle = \frac{1}{\sqrt{N}} |0^n\rangle T_k(1) |\widetilde{\pi}\rangle + \sqrt{\frac{N-1}{N}} |0^n\rangle T_k(1-\delta) |\widetilde{v}\rangle + |\bot\rangle, \qquad (7.21)$$

where  $|\perp\rangle$  is an unnormalized state satisfying  $(|0^n\rangle\langle 0^n|)\otimes I_n|\perp\rangle=0$ . Since  $T_k(1)=1$  for all k, we have

$$p(0^n) = \frac{1}{N} + \left(1 - \frac{1}{N}\right) T_k^2 (1 - \delta). \tag{7.22}$$

Using the fact that  $T_k(1-\delta) = \cos(k\arccos(1-\delta))$ , we can show that  $T_k(1-\delta) \approx 0$  when k satisfies

$$k \approx \frac{\pi}{2\arccos(1-\delta)} \approx \frac{\pi}{2\sqrt{2\delta}} = \frac{\pi\sqrt{N}}{2\sqrt{2}}.$$
 (7.23)

Therefore, after taking  $k = \lceil \frac{\pi \sqrt{N}}{2\sqrt{2}} \rceil$  steps of the quantum walk, the probability of successfully measuring  $|0^n\rangle$  drops down to 1/N, which is significantly lower than 1. This will allow us to declare with high confidence the presence of a marked vertex in the graph in  $\mathcal{O}(\sqrt{N})$  steps of a quantum walk, which is a significant (quadratic) speed up compared to  $\mathcal{O}(N)$  steps of a random walk required in the classical setting for large N.

We simulate this experiment for n=6 qubits in QCLAB. The script to reproduce this simulation is made available on https://github.com/QuantumComputingLab/qclab. We first generate quantum circuits that block encode the discriminant matrix for (7.15) and (7.16). These circuits are given in Figure 23.

Starting from the state (7.17), we repeat both circuits for k steps and measure the the success probability (7.18). The results of this simulation are shown in Figure 24. We observe that it is sufficient to use a very small k to distinguish the two states, and the two states are maximally distinguishable for  $k_{opt}$  given by (7.23) as indicated by the dotted line.

## References

Guang Hao Low and Isaac L. Chuang. Optimal hamiltonian simulation by quantum signal processing. *Phys. Rev. Lett.*, 118:010501, 2017.

Guang Hao Low and Isaac L Chuang. Hamiltonian simulation by qubitization. Quantum, 3:163, 2019.

András Gilyén, Yuan Su, Guang Hao Low, and Nathan Wiebe. Quantum singular value transformation and beyond: exponential improvements for quantum matrix arithmetics. In *Proceedings of the 51st Annual ACM SIGACT Symposium on Theory of Computing*, pages 193–204, 2019.

Lin Lin and Yu Tong. Optimal quantum eigenstate filtering with application to solving quantum linear systems. *Quantum*, 4:361, 2020a.

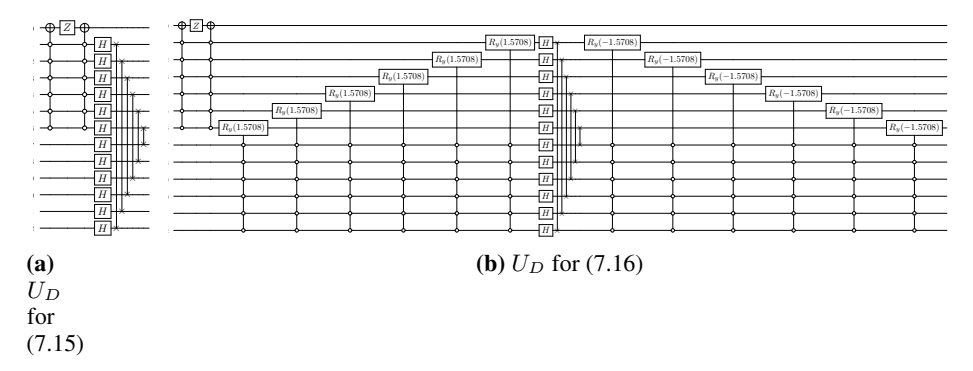


**Figure 23.** Quantum circuits for block-encoding of (7.15) and (7.16).

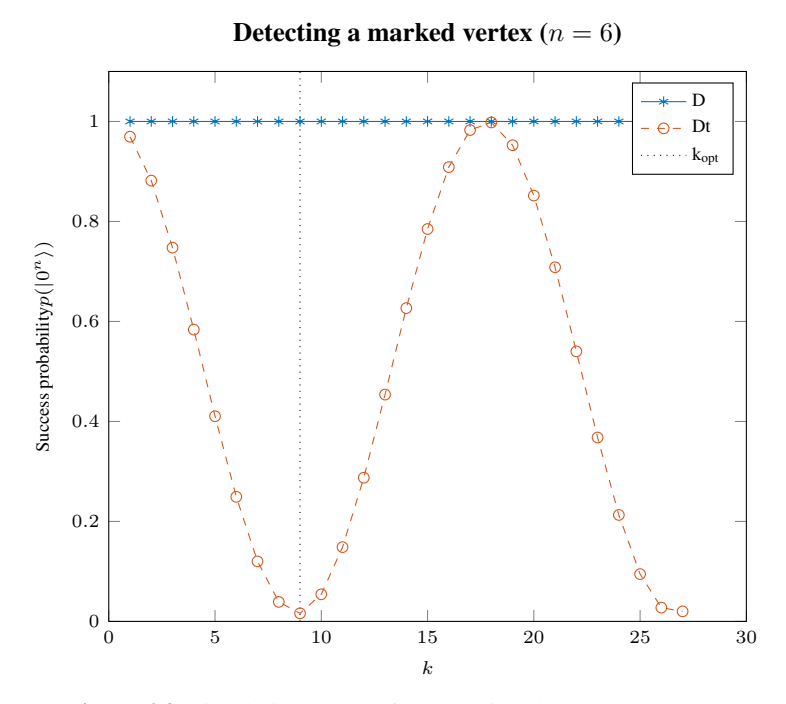


**Figure 24.** Simulation results for detecting the marked vertex.

Lin Lin and Yu Tong. Near-optimal ground state preparation. *Quantum*, 4:372, 2020b.

John M Martyn, Zane M Rossi, Andrew K Tan, and Isaac L Chuang. Grand unification of quantum algorithms. *PRX Quantum*, 2(4):040203, 2021.

Nai-Hui Chia, András Gilyén, Tongyang Li, Han-Hsuan Lin, Ewin Tang, and Chunhao Wang. Sampling-based sublinear low-rank matrix arithmetic framework for dequantizing quantum machine learning. In *Proceedings of the 52nd Annual ACM SIGACT symposium on theory of computing*, pages 387–400, 2020.

Ewin Tang. Quantum principal component analysis only achieves an exponential speedup because of its state preparation assumptions. *Phys. Rev. Lett.*, 127(6):060503, 2021.

Sevag Gharibian and François Le Gall. Dequantizing the quantum singular value transformation: Hardness and applications to quantum chemistry and the quantum pcp conjecture. *arXiv preprint arXiv:2111.09079*, 2021.

Dominic W. Berry, Andrew M. Childs, and Robin Kothari. Hamiltonian Simulation with Nearly Optimal Dependence on all Parameters. *Proceedings - Annual IEEE Symposium on Foundations of Computer Science, FOCS*, 2015-Decem: 792–809, 2015. doi:10.1109/FOCS.2015.54.

Andrew M. Childs, Robin Kothari, and Rolando D. Somma. Quantum algorithm for systems of linear equations with exponentially improved dependence on precision. *SIAM J. Comput.*, 46(6):1920–1950, 2017. doi:10.1137/16M1087072.

- Mario Szegedy. Quantum Speed-Up of Markov Chain Based Algorithms. In 45th Annual IEEE Symposium on Foundations of Computer Science, pages 32–41, 2004. doi:10.1109/FOCS.2004.53.
- Andrew M. Childs. On the relationship between continuous- and discrete-time quantum walk. *Comm. Math. Phys.*, 294 (2):581–603, 2010. doi:10.1007/s00220-009-0930-1.
- J. Haah. Product decomposition of periodic functions in quantum signal processing. Quantum, 3:190, 2019.
- Yulong Dong, Xiang Meng, K Birgitta Whaley, and Lin Lin. Efficient phase factor evaluation in quantum signal processing. *Phys. Rev. A*, 103:042419, 2021.
- Eleanor G Rieffel and Wolfgang H Polak. Quantum computing: A gentle introduction. MIT Press, 2011.
- T D Mackay, S D Bartlett, L T Stephenson, and B C Sanders. Quantum walks in higher dimensions. *Journal of Physics A: Mathematical and General*, 35(12):2745–2753, 2002. doi:10.1088/0305-4470/35/12/304.
- S.E. Venegas-Andraca. Quantum walks: a comprehensive review. Quantum Inf Process, 11:1015–1106, 2012.
- Neil Shenvi, Julia Kempe, and K. Birgitta Whaley. Quantum random-walk search algorithm. *Phys. Rev. A*, 67:052307, 2003. doi:10.1103/PhysRevA.67.052307.
- G. Paparo and Martin-Delgado M. Google in a quantum network. Sci Rep, 2:444, 2012.
- Juha J Vartiainen, Mikko Mötiönen, and Martti M Salomaa. Efficient decomposition of quantum gates. *Phys. Rev. Lett.*, 92(17):1–4, 2004. doi:10.1103/PhysRevLett.92.177902.
- T Loke and J B Wang. Efficient quantum circuits for Szegedy quantum walks. *Ann. Physics*, 382:64–84, 2017. doi:10.1016/j.aop.2017.04.006.